SAND2007-5059C

STATISTICS OF THE HUGONIOT ELASTIC LIMIT FROM LINE VISAR

Michael D. Furnish, Tracy J. Vogler, C. Scott Alexander, William D. Reinhart, Wayne M. Trott and Lalit C. Chhabildas

Sandia National Laboratories, M S 1168, PO Box 5800, Albuquerque NM 87185, USA

Abstract. Material heterogeneity appears to give rise to variability in the yield behavior of ceramics and metals under shock loading conditions. The line-imaging VISAR provides a way to measure this variability, which may then be quantified by Weibull statistics or other methods. Weibull methods assign a 2-parameter representation of failure phenomena and variability. We have conducted experiments with tantalum (25 and 40 μm grains) and silicon carbide (SiC-N with 5 μm grains). The tantalum HEL variability did not depend systematically on peak stress, grain size or sample thickness, although the previously observed precursor attenuation was present. SiC-N HEL variability within a single shot was approximately half that of single-point variability in a large family of shots; these results are more consistent with sample-to-sample variation than with variability due to changing shot parameters.

Keywords: HEL, strength, tantalum, silicon carbide, line VISAR, line ORVIS, Weibull statistics.
PACS: 62.50.+p, 07.60.Ly.

INTRODUCTION

The dynamic properties of bcc metals such as tantalum, and of hard ceramics such as silicon carbide (SiC-N) have been of interest for some time because of the high strength of these materials. Tantalum is also unique in its combination of large density, refractory properties, weldability and high thermal conductivity [1]. SiC is unique in its high strength to weight ratio.

In another portion of this study [2] we examined the spatial variability in the spall strength of two well-characterized tantalum samples, making use of the line-imaging VISAR [3,4]. The present study focuses on the spatial variability of the Hugoniot Elastic Limit, or HEL, both for the same tantalum materials as before and for SiC-N.

As with spallation, variability in the HEL is a consequence of material inhomogeneity, such as different crystallographic orientations, grain boundaries, small voids, and material impurities.

The present measurements utilize a time- and spatially-resolved interferometric diagnostic (line-imaging VISAR) to map out the velocity $v(y,t)$ of all points on a line on the free surface of a sample [3]. Here, y is a spatial coordinate (position on the line) and t is time. The time range of interest is that during the arrival of the loading waveform.

SAMPLES AND EXPERIMENTS

Two varieties of tantalum were tested. "AFRL Tantalum," which was obtained from Eglin Air Force Base, was processed to yield a uniform refined grain structure (grain size ~20 microns) with a strong axisymmetric [111] crystallographic texture. "LANL tantalum" was processed to yield a

more equiaxial structure with an average grain size of 42 microns. This material is the same as used by Gray *et al.* [4], who describe the texture strength as moderate ([111] component approximately eight times random). Compositional details are given in reference [2].

The SiC-N samples were manufactured by Cercom, and had a grain size of approximately 4 microns. They were of the 6H (hexagonal) polytype, with nominal density of 3.227 gm/cm^3.

The shot matrix (Table 1) was chosen to provide a range of Hugoniot stresses and sample thicknesses.

Table 1. Shot matrix

Shot #	Ta Impactor* mm thick ×dia	Ta Target mm thick × dia	Impact Vel. km/s	Nominal Stress GPa
		AFRL Tantalum		
Linr-4	0.246 × 42	1.148 × 42	0.402	12.2
Linr-6	0.203 × 42	4.488 × 42	0.396	12
Linr-10	0.216 × 21	4.491 × 42	0.393	12
Linr-12	3.393 × 42	4.509 × 42	0.205	6
Linr-13	1.440 × 42	3.0175 × 42	0.295	8.8
Linr-14	1.582 × 43	3.0505 × 42	0.396	12.0
		LANL Tantalum		
Ta-4	0.505 × 27	1.770 × 38	0.268	8
Ta-5	0.521 × 27	1.765 × 38	0.315	9.4
Ta-6	0.526 × 27	1.763 × 38	0.361	10.9
Ta-7	0.396 × 27	1.641 × 38	0.241	7.1

* Approx. 8 mm of C foam back the impactor on all experiments.

Shot #	Ta Impactor* mm thick ×dia	SiC Target‡ mm thick × dia	Impact Vel. km/s	Nominal Stress GPa
		SiC-N		
495	3.121 × 51	5.606 × 38	0.765	20

‡Target backed by 25 mm LiF window (51 mm dia.)

METHOD OF CALCULATING THE HEL

The longitudinal stress at the HEL is calculated as $\sigma_{xx(HEL)} = (1/2)\ \rho_0 \cdot U_{plat} \cdot U_{s(HEL)}$, where U_{plat} is the observed free surface interface velocity immediately after arrival of the elastic wave, which is approximately twice the *in-situ* material velocity behind the elastic wave., and $U_{s(HEL)}$ is the elastic wavespeed ($\approx C_l$). The yield strength may then be written as $Y = \sigma_{xx(HEL)} \cdot (1-2\nu) / (1-\nu)$, where is the Poisson's ratio ($\nu = 0.301$ for tantalum; 0.163 for SiC).

However, for actual waveforms, choosing U_{plat} and $U_{s(HEL)}$ may not be simple or unambiguous. For the tantalum samples, the method depicted in Fig. 1 was found to be applicable in most cases. In this method, for each position on the illuminated line (i.e. each value of y), a line segment is drawn extrapolating from two points on the ramp below the HEL, and a second is drawn extrapolating from a similar pair of points on the plateau following the HEL breakaway. The intersection is taken as the position of the elastic wave arrival. Finally, the entire wave is timeshifted so that the mean velocity of the elastic wave is equal to the nominal value of $C_l = (4.146+0.0291 \times \sigma_{HEL}\ (\text{GPa}))$ km/s [5].

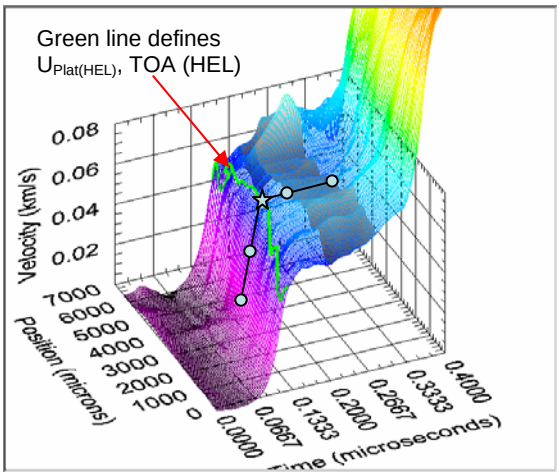

Figure 1. Method of choosing HEL for tantalum shots (case of Linr-12).

For the case of the SiC-N test 495, the only one of the four SiC-N tests we conducted which was at a stress level above the HEL, the streak camera record (Fig. 2 top) showed a very sharp loading to the HEL condition, followed by a ramp to the final state. Qualitatively the fringe motion mimics the velocity history; this is used for illustration purposes here. The elastic wave apex at each point was taken as where the sharp rise terminated (Fig. 2b).

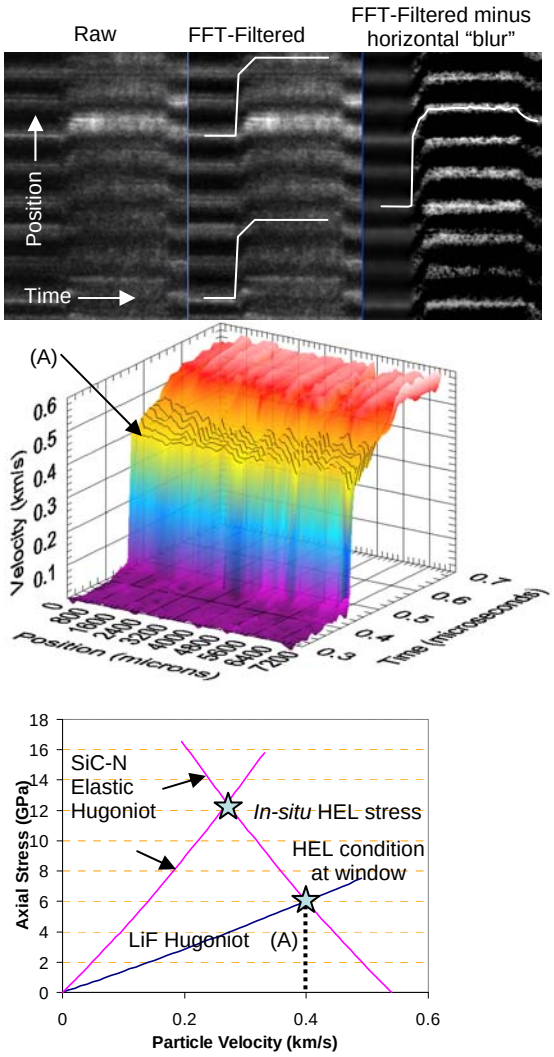

Figure 2. SiC-N Experiment 495. (Top) Portion of streak record showing processing and illustrating location of elastic jump. (Middle) Velocity surface; (A) is interpreted as the HEL wave. (Bottom) Impedance match method for calculating in-situ HEL axial stress (note that this does NOT give the Hugoniot condition).

WEIBULL ANALYSIS FOR Ta

It is the variability in material strength that gives rise to variability in the HEL. Failure statistics are customarily described by a Weibull function [6], which is based on the weakest-link theory. The cumulative probability distribution for failure at or below a given stress σ is given by $P(\sigma) = 1 - \exp[-(\sigma / \sigma_0)^m]$, where m is the Weibull modulus and σ_0 is a scale parameter with the same dimensions as σ [7]. Here, a plot of $\ln\{\ln[1/(1 - P)]\}$ against $\ln(\sigma)$ has slope m. The probability of failure P is found by ordering the results from lowest to highest spall strength, and assigning the jth result in a series of n measurements a failure probability P_j, which can be approximated [7] as $P_j = (j\text{-}0.5)/n$. For Ta-12, the results are shown in Figure 3(a), along with a linear fit.

The Weibull modulus m is large for a relatively uniform material failure response, and small if there is a wide range of spall strengths measured. The scale parameter σ_0 may be calculated as $\sigma_0 = \exp(-b/m)$, where the fit to the plot in Fig. 3 is $y = mx + b$. This represents that point of the failure distribution where a fraction $P(\sigma = \sigma_0) = 1\text{-}e^{-1}$ of the points on the line have failed, and is a value for the yield strength of the material. The resultant yield distribution is plotted against the histogram in Fig. 3(c). Note that the Weibull analysis is *not* a fit to the histogram.

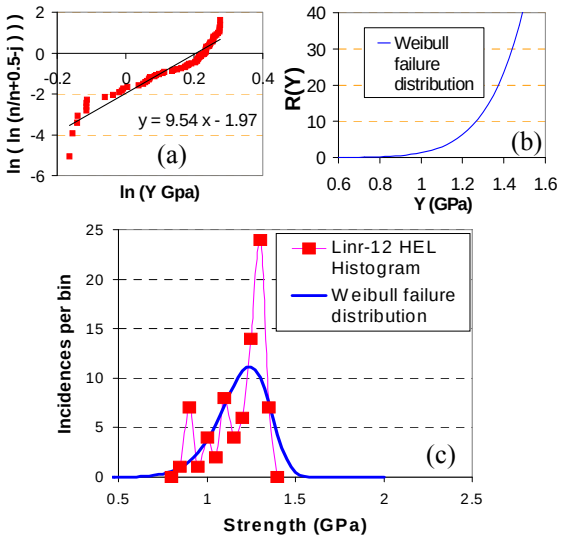

Figure 3. Wiebull analysis for loading failure (Linr-12). (a) Linear fit of failure data; (b) Failure rate R(Y) as a function of Y; (c) Resultant failure distribution, plotted against observed histogram of yield strength Y.

Table 2 summarizes the results of repeating this process for all of the tantalum tests.

Table 2. Weibull characterization of yield strength

Shot name	Sample Type	*m*	σ_0* GPa	Thickness mm	Stress GPa
Linr-4	AFRL	9.402	1.902	1.148	12.2
Linr-6	AFRL	7.180	1.263	4.488	12
Linr-10	AFRL	9.001	1.214	4.491	12
Linr-12	AFRL	9.539	1.230	4.501	6
Linr-13	AFRL	4.155	1.401	3.017	8.8
Linr-14	AFRL	3.803	1.678	3.050	12
Ta-4	LANL	6.634	1.238	1.770	8
Ta-5	LANL	8.662	1.139	1.765	9.4
Ta-6	LANL	5.548	1.342	1.763	10.9
Ta-7	LANL	6.474	1.508	1.641	7.1

*The HEL is approx. $1.758\sigma_0$ ($\nu = 0.301$).

We do not note any significant correlations between the variability coefficient *m* and any of the independent quantities (sample type, final stress and sample thickness). However, for the AFRL tantalum (which employed a range of thicknesses), the yield stress decreases with sample thickness ($Y=2.14$ GPa $- 0.2$ GPa/mm $\times X$; $R^2 = 0.9$).

SiC-N ANALYSIS

Of particular interest is how the statistical spread in one shot compares with the spread in a family of single-point shots. We compare the Weibull results from the SiC-N shot 495 with those from a family of shots from Vogler et al. [8] in Fig. 4. Note that the variations monitored here due to variations in surface velocity are approximately

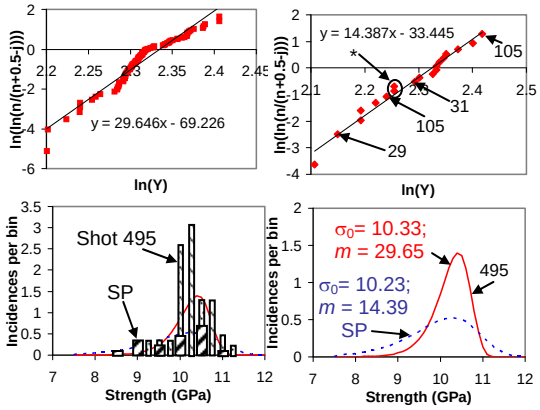

Figure 4. SiC-N yield strength distributions. (a) Line VISAR; (b) Single point series from [8]; numbers are Hugoniot stresses; *=6 mm samples vs. 3 mm; (c) histogram of strengths (SP=single point); (d) Weibull results

twice the maximum variations due to the $\pm < 25$ ns variation in the elastic wave arrival time.

The distribution of strengths from the multi-shot series is approximately twice as wide as from the single 7 mm length line. However, this is apparently not due to variations in shock amplitude or even sample thickness (cf. Fig. 4(b)). All of these shots were drawn from the same source; apparently inter-sample variability is greater that variability within a single sample.

ACKNOWLEDGEMENTS

Sandia is a multiprogram laboratory operated by Sandia Corporation, a Lockheed Martin Company, for the United States Department of Energy's National Nuclear Security Administration under Contract DE-AC04-94AL85000.

REFERENCES

1. Koch, W. and Paschen, P, Tantalum- Processing, Properties and Applications, J. Metals, vol. 41, pp. 33-39, 1989.
2. Furnish, M.D., Chhabildas, L.C., Reinhart, W.D., Trott, W.M. and Vogler, T.J., Determination of Statistics of Microstructural Effects in Spalled Tantalum from 7 to 13 GPa, submitted to Intl. J. Plasticity
3. Trott, W. M., Knudson, M.D., Chhabildas, L.C. and Asay, J.R., Measurements of spatially resolved velocity variations in shock-compressed heterogeneous materials using a line-imaging velocity interferometer, in M. D. Furnish, L. C. Chhabildas and R. S. Hixson, Shock Compression of Condensed Matter - 1999, AIP Press, pp. 993-996, 2000.
4. Bloomquist, D. D. and Sheffield, S. A., "Optically recording interferometer for velocity-measurements with subnanosecond resolution," J. Appl. Phy., 54, 1717-1722, 1983.
5. Guinan, M.W. and Steinberg, D.J., Pressure and temperature derivation of the isotropic polycrystalline shear modulus for 65 elements, J. Phys. Chem. Sol., 35, 1501, 1974
6. Weibull, W., *J. Appl. Mech, 18*, 293, 1951
7. O'Sullivan, J.D. and Lauzon, P.H., Experimental probability estimators for Weibull plots, *J. Mat. Sci Let., 5*, 1245-1247, 1986.
8. Vogler, T.J.; Reinhart, W.D.; Chhabildas, L.C.; Dandekar, D.P., Hugoniot and strength behavior of silicon carbide, J. Appl. Phys., 99, 1-15, 2006.